

# Synchronization Cost of Coupled Oscillators With a Spatial Embedding

KORAY ÇİFTÇİ 

Biomedical Engineering Department, Çorlu Faculty of Engineering, Tekirdağ Namık Kemal University, 59860 Tekirdağ, Turkey

e-mail: kciftci@nku.edu.tr


**ABSTRACT** Synchronous behavior brings advantages for complex systems. Yet, this advantage comes with a cost: Emergence and sustainability of synchronization requires a continuous exchange among the interacting units. Thus, networks with optimal synchronization dynamics is a subject of active research. In this study, we define a cost function for synchronization which takes into account both the network structure which is embedded in space and the dynamic coupling within the system. Beginning from a fully connected network and using an edge pruning strategy based on simulated annealing, we searched for optimal configurations for synchronization with minimum cost. We observed that the same levels of synchronization with a fully connected network can be reached by different networks with sparse connections. We conclude that the chain structure, clustering behavior and degree-frequency relations are the main determinants of optimally synchronizable network structures.

**INDEX TERMS** Complex systems, Kuramoto model, oscillator, network, synchronization.

## I. INTRODUCTION

Synchronization is ubiquitous in nature. Synchrony among individuals is essential for the harmony and sustainability of the social systems [1], [2]. On the other hand, message and information passing might be optimized via synchronization in biological systems [3]. Nonetheless, synchronization is a costly process, since it requires a continuous exchange of information, material etc. between the units of complex systems. Thus, if synchronous behavior is a common theme among living systems, then it should have brought an evolutionary advantage over selective pressures. And in the sequel, this should have been accomplished in an optimal way in terms of energy expenditure and resource allocation.

Topological structure plays a central role in the synchronizability of a complex network [4], [5]. Previous research has shown that synchronizability of a complex network is dependent on the effective coupling among oscillators [6], and synchronization is enhanced in weighted networks where weighting procedure depends on the global network structure [7]. Adaptively updating the coupling strengths based on the local synchronization properties also has a positive effect on the complete synchronization of the network [8].

The associate editor coordinating the review of this manuscript and approving it for publication was Weisi Guo .

In real world problems, optimizing synchronization under topological constraints is a major concern [9]. The synchronization cost of coupled systems has been investigated in a number of studies. Using a dynamic cost function, it was demonstrated that synchronization cost was minimized in a network topology with rich club organization [10]. In another study [11], by employing a rewiring based strategy, the wiring rules for optimal synchronization of a network of nonidentical oscillators were shown to be dependent on the native frequencies of the oscillators.

An analysis based on the Laplacian matrix of the graph of oscillators demonstrated that the synchronizability of the network depended on the mean degree of the nodes [12]. Using a cost function derived from this synchronizability concept, and introducing a spatial embedding for the network, it was shown that spatial clustering and network modularity were the main determinants of optimal configurations for synchronization [13].

In the current study, we will base our framework on the classical Kuramoto Model [14], with the addition of a spatial dimension. Kuramoto Model is a widely used model for analyzing the synchronization behavior of a system of interacting particles [15], [16]. It faithfully reproduces many of the synchronization related phenomena [17]. The model is built on a set of coupled oscillators whose states are represented by their phases. The model is simple and mathematically tractable,

yet it demonstrates enough complexity to generate various synchronization patterns [18].

The main contributions of this paper are as follows:

(1) To relate synchronization behavior to cost, we introduce a function which depends on the actual interactions between the oscillators as in [10], but which also takes into account spatial embedding as in [13]. Hence, we consider both the static and dynamic aspects of coupling. We calculate the static cost from the network structure and couple this with the dynamic cost which we calculate from the simulations running on this network.

(2) We use both discrete and continuous spatial coordinates.

(3) Rather than fixing the number of edges beforehand, we adopt a pruning based strategy, and start with a fully connected network. We employ a modified version of simulated annealing algorithm [19] and we prune the edges as long as the network can reach the same level of synchronization with less cost. Hence, our approach is more general than rewiring based strategies.

(4) We make a comprehensive analysis regarding the interplay between synchronization, coupling cost and network structure by employing the techniques of graph analysis.

The rest of the paper is organized as follows: We first present a short summary of the Kuramoto Model. Then we define a spatial embedding for the oscillators and introduce the function that we will use to measure synchronization cost. After explaining the basic graph notions that we will need to characterise the networks, we will place the oscillators on a fully coupled network and observe its evolution by pruning the edges with the condition of decreasing the cost for synchronizability. The results concerning the relationships between synchronization dynamics and network structure will be followed by our conclusions from these results.

## II. METHODS

### A. KURAMOTO MODEL WITH A SPATIAL EMBEDDING

The Kuramoto model takes each unit of a multi-particle system as an oscillator whose state is defined solely by its angular phase ( $\theta_n$ ). Each particle has an intrinsic angular frequency ( $\omega_n$ ). Accordingly, the oscillators rotate at their own pace when there is no coupling among them. In this study, we place  $N$  oscillators on the nodes of a graph. The topology of the graph determines the connectivity between the nodes. Kuramoto model places a coupling function among the oscillators which is a function of the phase difference between the oscillators:

$$\dot{\theta}_n = \omega_n + \frac{K}{\langle k \rangle} \sum_m a_{mn} \sin(\theta_m - \theta_n) \quad (1)$$

where,  $a_{mn}$  is 1 if there is an edge between the nodes  $m$  and  $n$ , (i.e. node  $m$  is a neighbor of node  $n$ ), 0 otherwise.  $K$  is the constant determining the coupling strength,  $\langle k \rangle$  is the average degree of the graph. In this model, each oscillator takes an input from its direct neighbors, and its instantaneous

frequency is determined by both its intrinsic frequency and the continuous input from the neighbors. Because of the choice of the interaction function, when the oscillators are completely in-phase or anti-phase, interaction function vanishes. However, in the anti-phase situation the phases repel each other, whereas when the oscillators are close to be in-phase they are pulled together. Thus, the model in whole creates a single stable attractor for the phases. The coupling strength  $K$  is the basic parameter that determines the behaviour of the oscillators. When this parameter is below a critical value, the oscillators mainly behave according to their intrinsic angular frequencies, whereas when this parameter approaches a critical value, oscillators are pulled together, and phase synchronization begins to emerge. In the original Kuramoto Model, where a complete graph is investigated, the coupling strength is normalized by the number of nodes,  $N$ . But in this study, we opted to normalize the coupling strength by average degree, since our pruning strategy will generate a heterogeneous degree distribution. It has been shown that this form of normalization makes the coupling strengths symmetric and weighs all links equally for non-globally coupled networks [20], [21].

Kuramoto Model gives us a measure for observing the synchronization behavior of the oscillators: The order parameter  $r$  and the average phase  $\psi$  represents the global synchronization of the oscillators:

$$r e^{i\psi} = \frac{1}{N} \sum_{j=1}^N e^{i\theta_j} \quad (2)$$

Actually,  $r$  corresponds to the vector sum of the oscillator phases distributed across the unit circle.  $r$  being close to 1 is an indicator of global synchronization. With the introduction of the order parameter, Eq. (1) may be re-written as,

$$\dot{\theta}_n = \omega_n + \frac{K}{\langle k \rangle} N r \sin(\psi - \theta_n) \quad (3)$$

This equation more clearly expresses the relationship between the mean field described by  $r$  and  $\psi$ , and individual oscillators: The oscillators whose intrinsic frequencies are lower (higher) than the average phase velocity will be accelerated (decelerated) to keep the oscillators at the same pace. If (1) is written for all oscillators and summed up, then,

$$\sum_n \dot{\theta}_n = \sum_n \omega_n \quad (4)$$

is obtained. This equation tells us that the total phase velocity of the system is constant and completely determined by the initial intrinsic frequencies of the oscillators. What changes as the model evolves is the distribution of this total velocity among the oscillators. With the emergence of synchronization, phase velocity of the oscillators converge and this common phase velocity may be written as,

$$\dot{\theta} = \frac{1}{N} \sum_{i=1}^N \omega_n, \quad (5)$$

Accordingly, all the oscillators in the group would begin to rotate at this velocity, and this is accomplished by the constant exchange of coupling between the oscillators, which is represented by the second term of Eq.(1). If we denote this second term as  $C_n$ , then Eq.(1) can be written as,  $\theta_n = \omega_n + C_n$ . Please note that, the global phase velocity of the oscillators given by Eq. (5) is also the minimizer of a cost function,  $C$ , which might be defined as,  $C = \frac{1}{N} \sum_{i=1}^N C_n^2$ . This gives us the intuition that the synchronization process might also be seen as the minimization process of the exchange cost among the interacting units. But it should be noted that the cost function defined above depends on the variance of the intrinsic frequencies of the oscillators. So, the initial variance of the oscillators determines the minimum value of this coupling cost.

In [10], a simple cost metric based on the phase difference between oscillators was proposed. Similarly, we will define the dynamic part of the cost function,  $J_d$ , directly from the coupling term in the model:

$$J_d = \sum_{m,n} a_{mn} \sin^2(\theta_m - \theta_n) \quad (6)$$

This function gives us the actual rate of exchange between the interacting particles. This interaction takes place in a network, and the cost of this network depends on two factors: The total length of wire to create this network (wiring cost) and the total signal carriage capacity of this network, which depends on  $K$ . About the latter, since  $K$  is normalized with  $\langle k \rangle$ , the total amount of coupling signal stays the same for all networks with the same number of nodes, regardless of the edge density. So, as the number of edges in a network decreases (increases), maximum amount of interaction signal running through the individual edges will increase (decrease). This is needed to make the networks with different number of edges comparable. To take into account the former factor, we will impose a spatial embedding for the graph of oscillators. This would allow us to define a distance metric. Thence, all of the interactions between the oscillators would take place on this spatial coordinate system, and the distance between the two oscillators,  $d_{mn}$ , is the length of the path that should be traversed to reach from one to the other. Thereby, we can now define a static cost function,  $J_s$ , between the oscillators:

$$J_s = \frac{K}{\langle k \rangle} \sum_{m,n} d_{mn}. \quad (7)$$

This function can be interpreted as the infrastructure cost. When the structure of a network is settled, the static part of the coupling cost is determined and the dynamic part will depend on the nodal dynamics, i.e. phases and phase velocities. The static and dynamic part of the cost can be brought together to define the total coupling cost:

$$J = \alpha J_d + (1 - \alpha) J_s, \quad (8)$$

where  $\alpha$  determines the relative weights of these cost functions.  $\alpha = 0$  will give a cost function which just depends on

the network structure, whereas  $\alpha = 1$  ignores the structural costs.

In this study, we employ two metric spaces for the graph: First one is discrete in which we place the oscillators randomly on a unit circle equidistantly. Thus,  $N$  nodes are placed  $1/N$  units apart, and all the connections between the nodes will be throughout this unit circle. The second metric space we use is continuous in which we place the oscillators randomly on a unit square plane. Accordingly, the distance between the oscillators will be given by the Euclidean distance between them.

## B. PRUNING STRATEGY

We will consider undirected graphs without any self loops. We start with complete graphs in which all the nodes are connected to each other. By choosing a suitable value for the coupling constant  $K$ , we calculate the order parameter  $r$  and the synchronization cost  $J$  for the complete network. Afterwards, we resort to a modified simulated annealing procedure as described in [19]: We remove randomly selected edges from the network. The number of the removed edges is randomly chosen from an exponential distribution. So, we get a candidate graph for next iteration. We reject this candidate graph if it is disconnected, i.e. if there are some nodes which are unreachable from the rest of the nodes. If the network is connected then we let the network evolve, and calculate the order parameter and the synchronization cost for this network. For this candidate graph to be acceptable, first of all, its order parameter should be greater than or equal to the complete graph. This requirement is for to ensure that the synchronization capacity of the network is not adversely affected as we remove the edges from the graph. If this requirement is met, then we check the synchronization cost. If this cost is less than the previously stored cost, then we accept this candidate graph. If the cost is the least cost that have been encountered during the simulations then we store it as the best cost and, the candidate graph as the best graph. If the cost is not less than the previous cost, then we accept the candidate with probability  $p = \min[1, 1 - (1 - q)\delta J/T]^{1/(1-q)}$  [22].  $\delta J$  is the cost difference,  $q$  is a parameter which we take as  $-3$  since this value was shown to give the fastest convergence rate [19], and  $T$  is the temperature parameter that controls the acceptance probability.

At the start of the simulations we kept the temperature at  $T = \infty$  for  $N$  iterations and, after  $N$  iterations we update  $T$  as  $T = (1 - q)\delta J_{max}$ . Afterwards, we decrease the temperature after each iteration that ended with an accepted graph, by multiplying  $T$  by  $0.98$ . If no successful pruning attempts could be made for  $5N$  iterations, then we randomly add  $N/2$  edges to the graph. We observed that re-adding previously deleted edges to the graph might be beneficial for the algorithm to better explore the edge combinations for cost minimization. We terminated the pruning process if there is no successful pruning attempts for  $10N$  iterations.

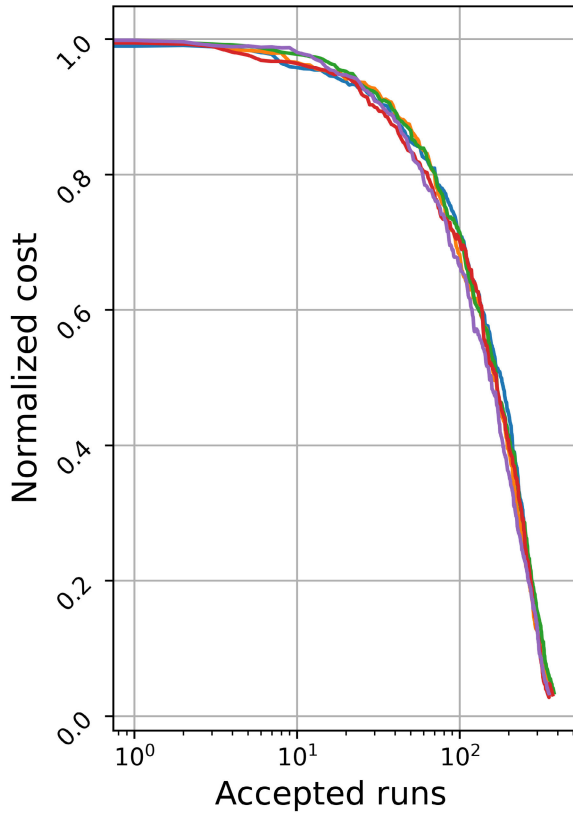


**FIGURE 1.** Normalized cost for different runs with the same initial network parameters. The figure shows the evolution of best cost. The same network parameters generates very similar final cost values.

**C. SIMULATIONS**

The simulations were all implemented on the *Python3* platform, using the custom written codes with the inclusion of *Networkx* package [23]. The network size was varied in the range (32, 64, and 96). Larger network sizes were tested but because of the computational complexity, full analyses were not implemented and only some representative values were collected. Here, we present the results for the networks with 96 nodes, but the results we have obtained for lower and higher network sizes were quantitatively very similar and qualitatively almost the same.

The initial phases of the oscillators were randomly selected from a uniform distribution between  $-\pi$  and  $\pi$ , and the initial angular velocities of the oscillators were randomly selected from unit normal distribution. We randomly selected the positions of the oscillators from the corresponding continuous and discrete coordinate systems.

During the simulations, after the initialization for each candidate pruned network, we evolved the oscillator phases according to the Kuramoto Model, using Euler approximation with time steps of 1 ms. We let the network evolve and calculate the statistics after the convergence of the order parameter.  $\alpha$  value was chosen as  $\alpha \in (1.0, 0.8, 0.6, 0.4, 0.2, 0.0)$  to observe the change in the network behavior with the change of the relative weights of static and dynamic costs.

**Normalized Cumulative Histogram**

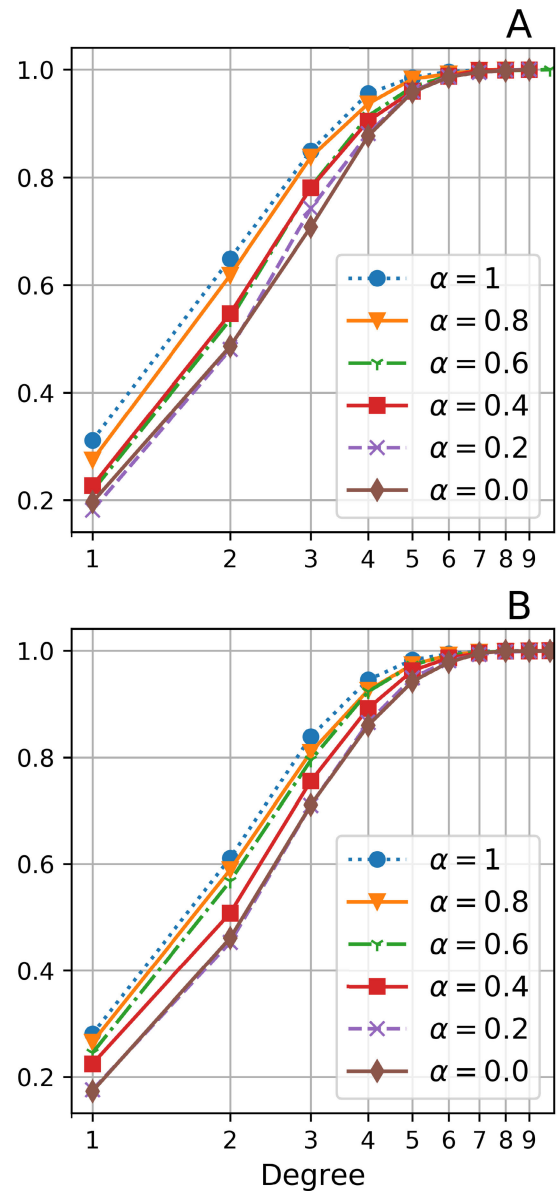


**FIGURE 2.** Normalized cumulative degree histogram for A) Square topology, B) Circular topology, for different values of  $\alpha$ . Node degree distribution becomes more homogeneous as dynamic costs gain importance.

For each value of  $\alpha$  we initialized the network 100 times and for each initialization we repeated the procedure for 10 times with the same initial values.

**III. RESULTS AND DISCUSSION**

**A. CONVERGENCE CHARACTERISTICS**

First question that we would like to answer was whether this procedure had given us consistent results or not. Since the dimension of the search space (number of combinations for edge pruning) is very high, it might not have been possible

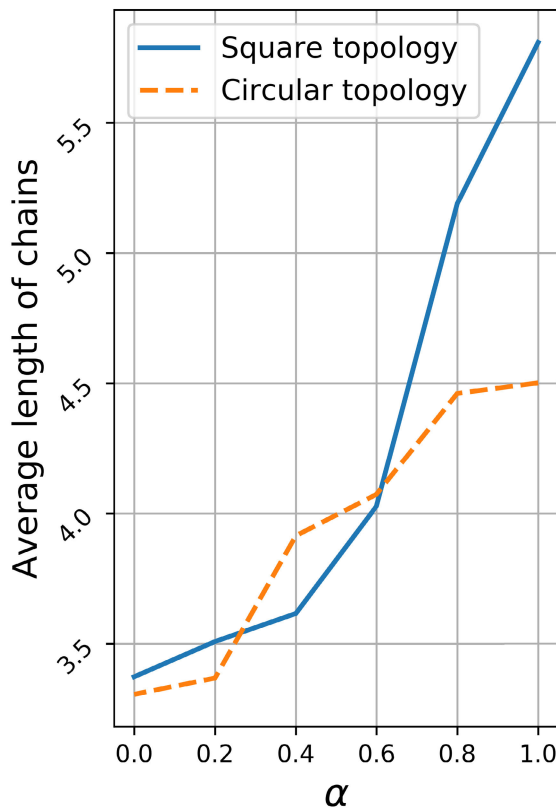


**FIGURE 3.** Average length of chains in the networks for different values of  $\alpha$ . As dynamic costs become more prevalent, number of high-degree nodes decreases and average length of chains in the network increases.

to end up with the same final network. Yet, if we arrive at networks with similar final costs then we might confidently deduce that for a given phase and coordinate distribution, our approach selects the networks which are synchronizable as efficiently as fully connected networks, but with the added advantage of less cost. To probe a light on this issue, we compared the variation of synchronization cost of ten networks for the same initial phase and coordinate values.

Figure 1 shows that although the path differs from trial to trial, the final networks has very similar costs. When we checked the edge-by-edge similarity of the networks, we couldn't observe high correlations between the networks. Hence, we can conclude that although the pruned networks are not exactly the same across trials, our pruning strategy returns us optimal networks in terms of synchronization. Thus, now the question is whether these networks exhibit some generalizable common structural properties or not.

### B. DEGREE DISTRIBUTIONS

Degree distribution of the nodes is a major factor determining the structure of a network. Therefore, we first compared the degree distributions of the networks obtained for each value of  $\alpha$ , where  $\alpha = 0$  corresponds to a fully static cost function, and  $\alpha = 1$  corresponds to a fully dynamic cost function. In Figure 2, it may be observed that as the relative weight shifts from static to dynamic, the normalized cumulative

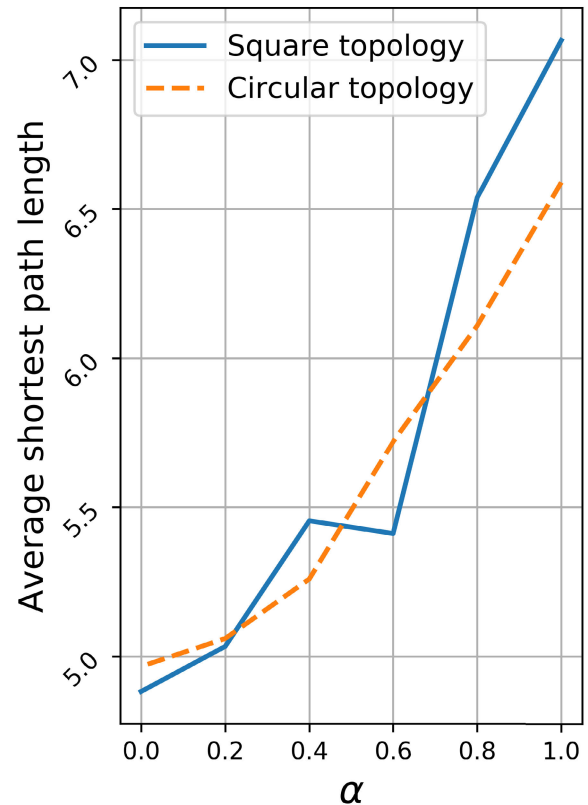


**FIGURE 4.** Average shortest path length with respect to  $\alpha$ . When the wiring costs are more dominant, network tries to minimize the path lengths during synchronization. As dynamic interactions begin to prevail, network prefers longer average path lengths. This is inline with the increase in the average length of chains.

probability distribution function shifts left, meaning that the number of high degree nodes decreases. This shift in degree distribution also reflects the change in the network structure: When static costs are more dominant central nodes with high degrees emerge which corresponds to a star-like pattern, whereas when the dynamic interactions between the nodes gain importance these high-degree nodes disappear with the network driven into a more chain-like structure. To be able to quantify this, we measured the average length of the chains in the networks. Figure 3 clearly demonstrates this trend. This shift in degree distribution is also an indication that node degrees become more homogeneous with increasing  $\alpha$ . It was earlier shown that homogeneity of the node degrees was better for the synchronizability of the networks [12].

### C. PATH LENGTH, CLUSTERING, AND BETWEENNESS

Average shortest path length and average clustering coefficient are the two main parameters used to characterize the structure of a network. Average shortest path length is the average shortest distance between all pairs of nodes in a network, and average clustering coefficient measures the average level of connectedness among the neighbors of nodes. This latter parameter gives information about the local structure of the network, whereas the former provides us with

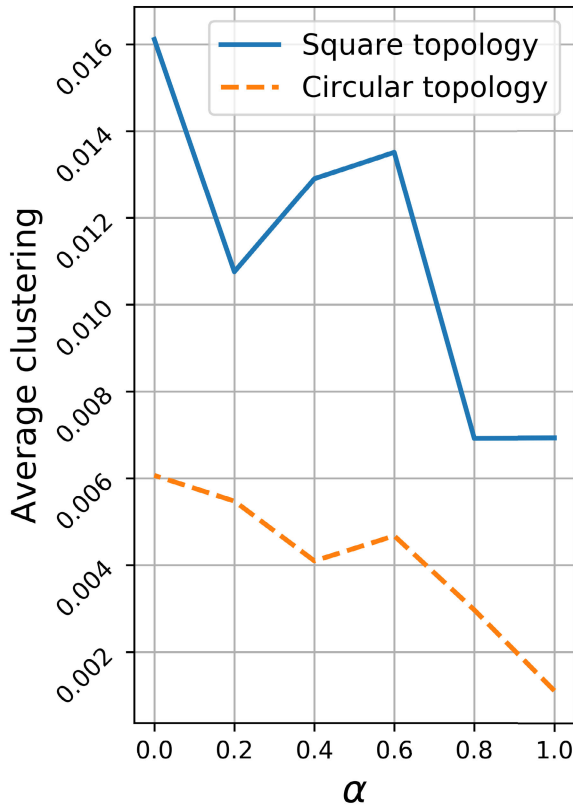


**FIGURE 5.** Average clustering with respect to  $\alpha$ . Nodes are driven into a more clustered structure when static costs are more determinant. This clustering behaviour disappears as dynamic aspects of the synchronization cost become more prominent.

an insight about the global structure. We naturally expect to see a decrease in path lengths as the network cost moves from dynamic to static and Figure 4 shows that this is indeed the case. The average clustering values for both topologies can be observed in Figure 5. Please note that because of the discrete nature of the circular topology, the coordinates of the oscillators stay fixed for all networks, but the intrinsic frequencies alter, whereas for square topology, since the coordinate system is continuous, both coordinates and intrinsic frequencies of the oscillators differ between networks. Thus, we might expect to have more statistical fluctuations for the square topology, and this is evident in the figures. Yet, for both coordinate systems, average clustering decreases for increasing values of  $\alpha$ . But, this decrease is not monotonic, and there is a local increase at around  $\alpha = 0.5$ . This shows that for low and high values of  $\alpha$ , the results are more consistent, but for intermediate values, where the dynamic and static costs are almost equally balanced the statistical uncertainty is higher.

The observed decrease in the average clustering coefficient means that when the wiring costs are ignored, oscillators exhibit a non-clustered behavior for optimal synchronization, but when wiring costs are included network tries to form a more clustered structure. Accordingly, the synchronizable networks with minimum wiring costs are characterized by

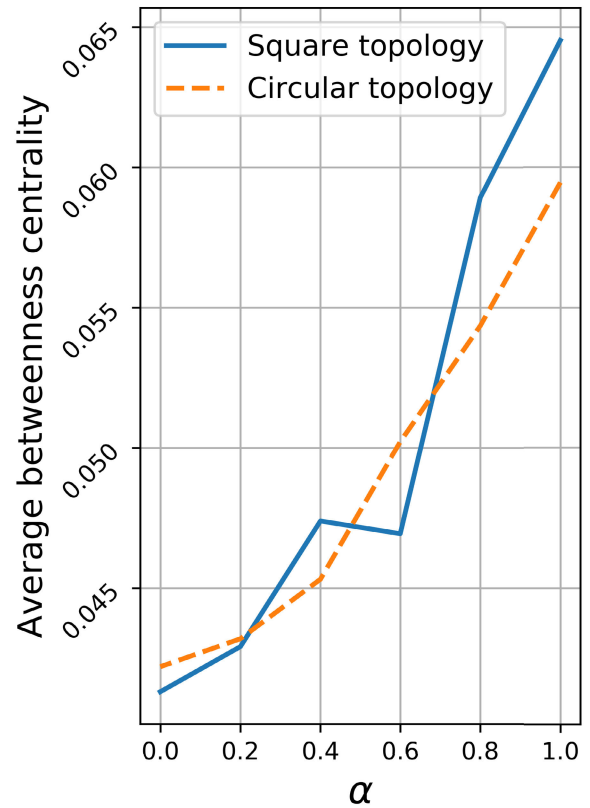


**FIGURE 6.** Average betweenness centrality increases for increasing values of  $\alpha$ . An increase in betweenness is preferred by the network to be able to minimize the cost of dynamic interactions between the oscillators. Betweenness values are given as percentages.

small average path lengths and high clustering coefficients. These results are in line with previous studies [13] and point to the fact that network structure evolves to a small-world topology in this case [24]. But when the actual dynamic couplings become more dominant then the path lengths increase and clusters disappear. It was earlier demonstrated that increased clustering hinders global synchronization [20].

A third measure that will highlight the structure of the cost optimized networks is the betweenness centrality. This parameter measures the number of shortest paths passing through a node. Previous studies have shown that betweenness centrality is inversely related with the static synchronization cost [19]. Here, we see a similar trend and observe that as the cost shifts from dynamic to static, betweenness centrality of the network decreases. (Figure 6).

#### D. DEGREE AND FREQUENCY

Previous studies investigated the frequency relationships between neighboring oscillators and it was found that adjacent oscillators should be anti-correlated for better synchronization [11]. A measure to quantify the correlation of frequencies between connected oscillators is given by [11]:

$$c_\omega = \frac{\sum_{i,j} a_{ij}(\omega_i - \langle \omega \rangle)(\omega_j - \langle \omega \rangle)}{\sum_{i,j} a_{ij}(\omega_i - \langle \omega \rangle)^2}. \tag{9}$$

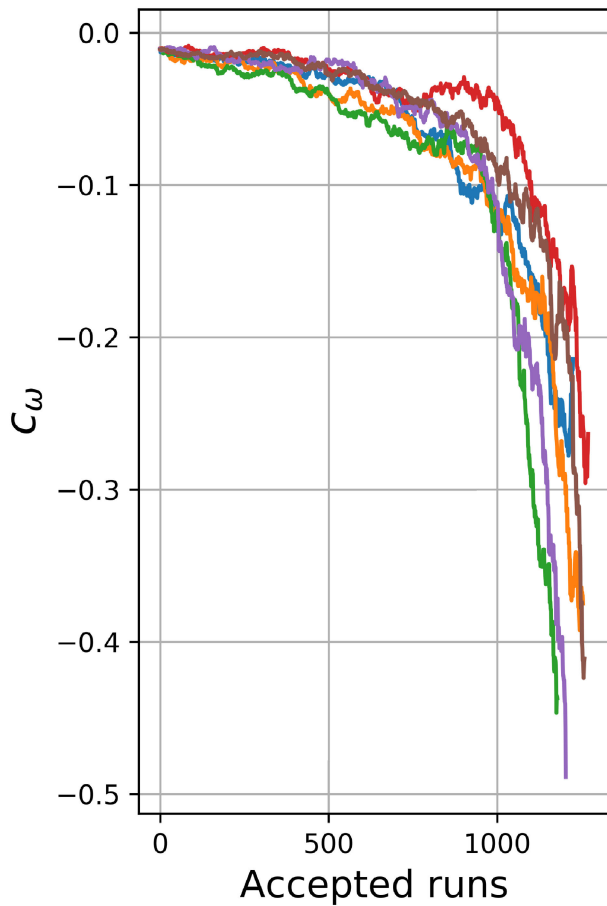


**FIGURE 7.**  $c_\omega$  measures the frequency correlation of neighboring oscillators. Nodes become anti-correlated as the network is driven into synchronization.

To see the evolution of this correlation measure during the pruning of edges, we recorded the cost and  $c_\omega$  during simulations. Figure 7 shows a sample of these simulations and demonstrates that decrease in cost goes along with an increase in the anti-correlation between adjacent nodes. Thus, connecting oscillators with opposite frequency signs decreases the synchronization cost of the network. We obtained similar results for all networks and for all  $\alpha$  values, and we couldn't observe any significant dependence on the  $\alpha$  values.

Another point that we would like to highlight is the relationship between node degree and frequency. It has been observed that synchronizable networks demonstrate a positive correlation between degree and frequency magnitude [11]. To this end, we calculated the Pearson's correlation coefficient between the degree of nodes and their frequency magnitudes. Figure 8 shows the average values of this correlation. First observation is that this correlation is always positive and it is higher for the square topology especially for  $\alpha$  values less than 0.5. And the highest values for this correlation is obtained for intermediate values of  $\alpha$ .

An important consideration in the investigation of network structures is the degree assortativity. This parameter

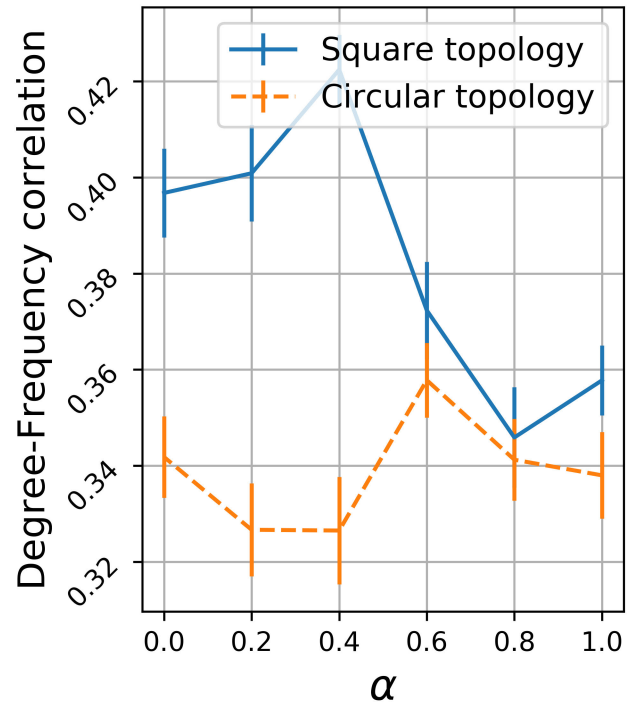


**FIGURE 8.** Average correlation coefficient between degree and node frequency magnitude is always positive for both topologies. High frequency nodes have higher degrees than the low frequency nodes.

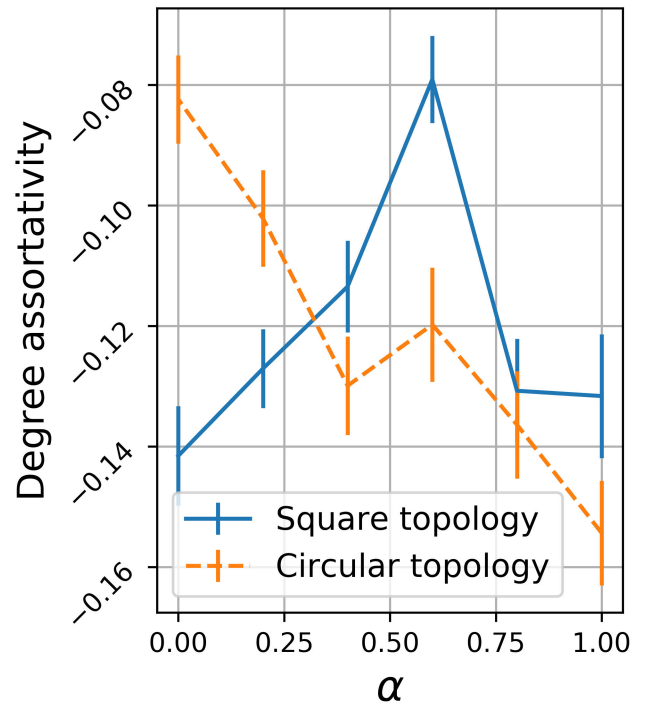


**FIGURE 9.** Average degree assortativity is negative for both topologies. High degree nodes are generally connected to low degree nodes and vice versa.

measures the preference of a node to attach to other nodes with similar degrees. Investigation of this parameter might supply us with additional knowledge on the synchrony cost optimized network structures. Figure 9 shows that minimal

cost synchronizable networks have small negative degree assortativity coefficients, meaning that the high (low) degree nodes of these networks generally prefer to make connections with low (high) degree nodes.

#### IV. CONCLUSION

Synchronization makes a major contribution to collective behavior. However, it is a costly process in terms of energy expenditure, and optimizing energy consumption is one of the major dimensions of evolution [25], [26]. The present study is an effort to understand the interplay between network structure, dynamics and synchronization cost.

We identified that amongst the synchronizable networks at the same level, small world networks are the ones that minimize the wiring cost. This was the cost that we labeled as the static cost in this study. However, when we introduced the dynamic aspects of the cost, i.e. actual couplings between the interacting elements, the minimal cost network diverged from small world connectivity and converged to a random connectivity profile [27].

We found that the balance of the static and dynamic parts of the cost function has a major effect on the resulting network structure, which exhibits itself in the homogeneity of the degree distributions, chain and path lengths, clustering and betweenness centrality.

Other major results of the current study is that there is an anti-correlation of frequencies between adjacent nodes and there is a positive correlation between node degree and frequency magnitude.

Some of these results have already been observed in previous studies. However, in those studies generally number of nodes and edges are fixed and a rewiring based strategy was applied to find optimally synchronizable network (e.g. [13], [19]). On the other hand, in the present work we have a very general approach: We started from a fully connected network, and pruned the edges as long as the network is synchronizable as good as the initial network, with less cost. Thus, we have the opinion that the results we present here will have a clarifying value to reveal the relationships between network structure and dynamics of complex synchronizable systems.

One of the possible directions for future work will be the exploration of the effect of more complex topological configurations, like Sierpinski networks [28], on the synchronization cost. Another line of research will be the investigation of biological networks, particularly brain networks. This is because brain regions have been shown to display neuronal synchronization [29], and also brain has been conjectured to be optimal in terms of wiring cost [30]. There are studies trying to adopt the Kuramoto Model to understand the synchronization in the brain [31]. Thus, exploring whether the brain is optimal or not in terms of synchronization cost will be informative for understanding the mechanisms of evident synchronization in the brain and other biological networks.

In this work, we present a basic graph theoretical analysis for understanding the interplay between network structure and synchronization. However, further research should employ more sophisticated tools of graph theory, like the identification of influential nodes in the network [32], [33]. By this way, it might be possible to build better connections between the local and global properties of networks and their synchronization profile.

#### REFERENCES

- [1] Z. Neda, E. Ravasz, Y. Brechet, T. Vicsek, and A.-L. Barabási, "The sound of many hands clapping," *Nature*, vol. 403, no. 6772, pp. 849–850, 2000.
- [2] K. Yun, K. Watanabe, and S. Shimojo, "Interpersonal body and neural synchronization as a marker of implicit social interaction," *Sci. Rep.*, vol. 2, Dec. 2012, Art. no. 959.
- [3] F. A. S. Ferrari, R. L. Viana, S. R. Lopes, and R. Stoop, "Phase synchronization of coupled bursting neurons and the generalized kuramoto model," *Neural Netw.*, vol. 66, pp. 107–118, Jun. 2015.
- [4] J. Lü, X. Yu, G. Chen, and D. Cheng, "Characterizing the synchronizability of small-world dynamical networks," *IEEE Trans. Circuits Syst. I, Reg. Papers*, vol. 51, no. 4, pp. 787–796, Apr. 2004.
- [5] X. Wang, "Complex networks: Topology, dynamics and synchronization," *Int. J. Bifurcation Chaos*, vol. 12, no. 5, pp. 885–916, 2002.
- [6] J. Gómez-Gardeñes, Y. Moreno, and A. Arenas, "Paths to synchronization on complex networks," *Phys. Rev. Lett.*, vol. 98, no. 3, 2007, Art. no. 034101.
- [7] M. Chavez, D.-U. Hwang, A. Amann, H. G. E. Hentschel, and S. Boccaletti, "Synchronization is enhanced in weighted complex networks," *Phys. Rev. Lett.*, vol. 94, no. 21, 2005, Art. no. 218701.
- [8] C. Zhou and J. Kurths, "Dynamical weights and enhanced synchronization in adaptive complex networks," *Phys. Rev. Lett.*, vol. 96, no. 16, 2006, Art. no. 164102.
- [9] T. Nishikawa and A. E. Motter, "Maximum performance at minimum cost in network synchronization," *Phys. D, Nonlinear Phenomena*, vol. 224, nos. 1–2, pp. 77–89, 2006.
- [10] T. Watanabe, "Rich-club network topology to minimize synchronization cost due to phase difference among frequency-synchronized oscillators," *Phys. A, Stat. Mech. Appl.*, vol. 392, no. 5, pp. 1246–1255, 2013.
- [11] M. Brede, "Synchrony-optimized networks of non-identical Kuramoto oscillators," *Phys. Lett. A*, vol. 372, no. 15, pp. 2618–2622, 2008.
- [12] A. E. Motter, C. Zhou, and J. Kurths, "Network synchronization, diffusion, and the paradox of heterogeneity," *Phys. Rev. E, Stat. Phys. Plasmas Fluids Relat. Interdiscip. Top.*, vol. 71, no. 1, 2005, Art. no. 016116.
- [13] M. Brede, "Small worlds in space: Synchronization, spatial and relational modularity," *EPL (Europhys. Lett.)*, vol. 90, no. 6, 2010, Art. no. 60005.
- [14] Y. Kuramoto, "Self-entrainment of a population of coupled non-linear oscillators," in *Proc. Int. Symp. Math. Problems Theor. Phys.* Berlin, Germany: Springer, 1975, pp. 420–422.
- [15] J. A. Acebrón, L. L. Bonilla, C. J. P. Vicente, F. Ritort, and R. Spigler, "The Kuramoto model: A simple paradigm for synchronization phenomena," *Rev. Mod. Phys.*, vol. 77, no. 1, p. 137, Apr. 2005.
- [16] F. A. Rodrigues, T. K. D. Peron, P. Ji, and J. Kurths, "The Kuramoto model in complex networks," *Phys. Rep.*, vol. 610, pp. 1–98, Jan. 2016.
- [17] S. H. Strogatz, "From Kuramoto to Crawford: Exploring the onset of synchronization in populations of coupled oscillators," *Phys. D, Nonlinear Phenomena*, vol. 143, nos. 1–4, pp. 1–20, 2000.
- [18] A. Arenas, A. Díaz-Guilera, and C. J. Pérez-Vicente, "Synchronization reveals topological scales in complex networks," *Phys. Rev. Lett.*, vol. 6, no. 11, 2006, Art. no. 114102.
- [19] L. Donetti, P. I. Hurtado, and M. A. Muñoz, "Entangled networks, synchronization, and optimal network topology," *Phys. Rev. Lett.*, vol. 95, no. 18, 2005, Art. no. 188701.
- [20] P. N. McGraw and M. Menzinger, "Clustering and the synchronization of oscillator networks," *Phys. Rev. E, Stat. Phys. Plasmas Fluids Relat. Interdiscip. Top.*, vol. 72, no. 1, 2005, Art. no. 015101.
- [21] Y. Moreno and A. F. Pacheco, "Synchronization of Kuramoto oscillators in scale-free networks," *EPL (Europhys. Lett.)*, vol. 68, no. 4, p. 603, 2004.



- [22] T. J. P. Penna, "Traveling salesman problem and Tsallis statistics," *Phys. Rev. E, Stat. Phys. Plasmas Fluids Relat. Interdiscip. Top.*, vol. 51, no. 1, p. R1, 1995.
- [23] A. A. Hagberg, D. A. Schult, and P. J. Swart, "Exploring network structure, dynamics, and function using NetworkX," in *Proc. 7th Python Sci. Conf. (SciPy)*, Pasadena, CA, USA, 2008, pp. 11–15.
- [24] D. J. Watts and S. H. Strogatz, "Collective dynamics of 'small-world' networks," *Nature*, vol. 393, no. 6684, pp. 440–442, 1998.
- [25] J. E. Niven and S. B. Laughlin, "Energy limitation as a selective pressure on the evolution of sensory systems," *J. Exp. Biol.*, vol. 211, no. 11, pp. 1792–1804, 2008.
- [26] A. Navarrete, C. P. van Schaik, and K. Isler, "Energetics and the evolution of human brain size," *Nature*, vol. 480, no. 7375, pp. 91–93, 2011.
- [27] H. Yamamoto, S. Kubota, F. A. Shimizu, A. Hirano-Iwata, and M. Niwano, "Effective subnetwork topology for synchronizing interconnected networks of coupled phase oscillators," *Frontiers Comput. Neurosci.*, vol. 12, p. 17, Mar. 2018.
- [28] T. Wen and W. Jiang, "An information dimension of weighted complex networks," *Phys. A, Stat. Mech. Appl.*, vol. 501, pp. 388–399, Jul. 2018.
- [29] M. V. L. Bennett and R. S. Zukin, "Electrical coupling and neuronal synchronization in the mammalian brain," *Neuron*, vol. 41, no. 4, pp. 495–511, 2004.
- [30] D. B. Chklovskii, T. Schikorski, and C. F. Stevens, "Wiring optimization in cortical circuits," *Neuron*, vol. 34, no. 3, pp. 341–347, Apr. 2002.
- [31] C. Lin and M.-M. Lin, "The mathematical research for the Kuramoto model of the describing neuronal synchrony in the brain," *Commun. Nonlinear Sci. Numer. Simul.*, vol. 14, no. 8, pp. 3258–3260, Aug. 2009.
- [32] T. Bian and Y. Deng, "Identifying influential nodes in complex networks: A node information dimension approach," *Chaos, Interdiscipl. J. Nonlinear Sci.*, vol. 28, no. 4, 2018, Art. no. 043109.
- [33] M. Li, Q. Zhang, and Y. Deng, "Evidential identification of influential nodes in network of networks," *Chaos, Solitons Fractals*, vol. 117, pp. 283–296, Dec. 2018.



**KORAY ÇİFTÇİ** received the B.S. degree in electronics engineering, in 1996, and the M.S. and Ph.D. degrees in biomedical engineering from Boğaziçi University, Turkey, in 2001 and 2008, respectively. He has been with the Biomedical Engineering Department of Tekirdağ Namık Kemal University, since 2009. His main research interests include neural signal acquisition and analysis, and computational neuroscience.

• • •